Chemometric Analysis of the Operation of PdO Thin Films as a Chemical Sensor for Ozone Molecules in the Atmosphere

© V.V. Chistyakov[1], S.V. Ryabtsev[2], A.A.K. Al-Habeeb[2], S.M. Soloviev[1], S.Yu. Turishchev[2]

[1] Ioffe Institute,
194021 St. Petersburg, Russia
[2] Voronezh State University,
394018 Voronezh, Russia

E-mail: v.chistyakov@mail.ioffe.ru

Received May 5, 2025
Revised June 24, 2025
Accepted September 18, 2025

Raw S and extracted S_{extr} conductivity responses of thin (30 nm) films of thermic palladium (II) p-type oxide under harmonic modulation of temperature T K were studied, and the temperature hysteresis of the S_{extr} and T was investigated. It is found that the dependences of S_{extr} on the ozone concentration of C ppb and the T K obey with good accuracy (adj $- R^2 > 0.995$) the Jovanovitch formula. For the first time a conductometric version of temperature-programmable desorption (TPD) of ozone ppb concentrations from PdO surface was applied. Based on the TPD-data, a conductometric analogue of the Wiegner-Polyani equation was specified, which monotonic with the C ppb parameters may serve as variates for multivariate calibration (MC) for selective ozone in atmosphere detection.

Keywords: temperature modulation, hysteresis, TPD, nonlinear regression, Wiegner−Polyani equation, multivariate calibration,selectivity.

DOI: 10.61011/SC.2025.07.62467.7793

Palladium oxide PdO thin films produced by various methods (see the review in Ref. [1]) are increasingly attracting the attention of specialists in the field of chemical gas sensors. In addition to its high catalytic activity, the material has p-type electrical conductivity at a hole concentration of $n_p \sim 10^{18}-10^{20}\,cm^{-3}$ [2], as well as high sensitivity to low concentrations of oxidizing gases such as ozone [3,4], chlorine and reducing gases — H_2, NH_3, CH_4, etc.

The prediction of the electrophysical, optical, and sensory properties of PdO in the framework of DFT (Density Functional Theory) calculations indicates that the material is a topological semimetal with the band intersections at both Dirac points and Weyl nodal lines and Fermi arcs and drumhead surface electronic states [5].

Previously, in order to increase the selectivity of sensors, the authors proposed a method for constructing the so-called multivariate calibration [6]. In multivariate calibration each analyte concentration is mapped to a vector, the components of which are obtained by nonlinear regression of the electrical conductivity signal on a set of so-called discriminating functions. An alternative multivariate calibration is proposed in this paper, which is based on the extracted [4] conductometric signal of the temperature-programmable desorption (TPD) and its specification based on the analog of the Wigner-Polyani equation (W−P), the concentration dependences of the parameters of which serve as calibration options.

Films of thermally oxidized palladium on polycore substrates with Pt contacts were used in the conducted experiments. The thickness of the films (~ 30 nm) corresponded to the maximum sensitivity to O_3 [3] at sensory-friendly film resistances of 1−3 kOhm. Measurements by the Van der Pauw method showed the following electrophysical characteristics in laboratory air at a humidity of 30−40 % for 2 samples at $t^\circ = 20\,^\circ$C: resistivity $7.377 \cdot 10^{-2}$ and $7.083 \cdot 10^{-2}$ Ohms · cm, hole concentration $6.274 \cdot 10^{18}$ and $6.682 \cdot 10^{18}\,cm^{-3}$, hole mobility 13.5 and 13.2 $cm^2 \cdot V/s$. As in the early studies [3,4], the authors recorded the electrical conductivity S during cyclic temperature changes of films according to the harmonic law with a period from 256 to 1024 s. Temperature cycling and measurement of the electrical conductivity response of the sensors were carried out using a computerized device with 1 °C temperature sampling. The time of the experiment for each ozone concentration is 2 h, i.e. ~ 30 thermal cycles at 256 s per cycle. This article presents the last four cycles with steady-state values of electrical conductivity. In this case, the reproducibility of the results from cycle to cycle is $\sim 1-2$ % in the almost complete absence of an evolutionary trend. This can be seen, for example, in Figure 1, where each graph is constructed using four thermal cycles.

Figure 1 shows the measured electrical conductivity S (mS) (Figure 1, a), as well as the extracted electrical conductivity S_{extr} (mS) (Figure 1, b), i. e., the difference between the response in the air flow with and without analyte. A special feature for all 4 studied ozone concentrations (25, 55, 90, and 250 ppb) was temperature hysteresis and self-intersections of curves (Figure 1, a and b), especially pronounced at 250 ppb.

The relationship of hysteresis with the moisture contained in the stream [4] was not confirmed, as this behavior was also observed in UHP argon (Figure 1, a). A discussion of the mechanism of the observed hysteresis is

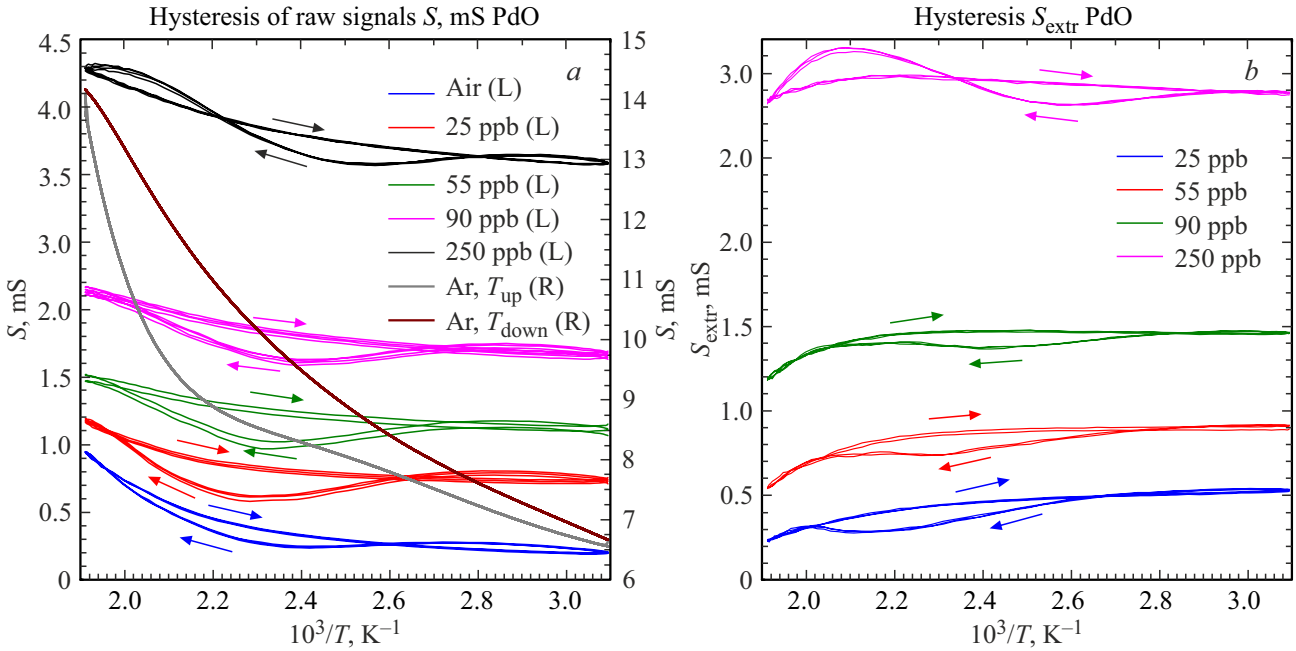

Figure 1. Temperature hysteresis of the electrical conductivity signals of the PdO film during cyclic temperature modulation: *a* — in UHP argon (right vertical axis) and in air with different concentrations of ozone (left vertical axis); *b* — extracted responses S_{extr} in air with ozone (decrease in temperature is indicated by arrows pointing to the right, increase is indicated by arrows pointing to the left).

beyond the scope of this article, but one of our several assumptions relates hysteresis to the imbalance of processes in the semiconductor-gas system, for example, as in the hydrodynamic mode of current transfer [7] with a sharp decrease/increase in carrier scattering.

Higher values of conductivity S (and its temperature variation) in neutral argon than in air containing acceptor molecules O_2 formally contradict the hole type of palladium oxide (II) conductivity. On the other hand, the authors of Ref. [2] also observed *n*-type of conductivity in this material explained by the presence of Pd clusters in the film. Also, to explain this, we can use the complex topological nature of current transfer in the volume and in the surface layer of PdO, predicted in Ref. [5].

The studied dependence for the half-sum of signals from ozone in the air at the stages of heating and cooling $S_{\text{av}} = 0.5(S_{\text{extr}\uparrow} + S_{\text{extr}\downarrow})$ of all known adsorption equations (Langmuir, Freundlich, Temkin, BET, etc.) is best described with adj $- R^2 = 0.996$ by the Jovanovich formula [8], but modified to take into account the effect of adsorption on the partial carrier mobility (associated with the analyte chemisorbed on the surface) μ_{part}:

$$S_{\text{extr.av}}(C, T) = A\left(1 - \exp\left(-bC\exp\left(\frac{Q}{RT}\right)\right)\right) \times \left(1 + WT^{\alpha}\left(1 - \exp\left(-bC\exp\left(\frac{Q}{RT}\right)\right)\right)\right), \quad (1)$$

where Q is the heat of adsorption; $R = 8.31\,\text{J/mol}\cdot\text{K}$; A, b, W, α are parameters (Figure 2, *a*).

The authors justify the use of this formula, derived for physical adsorption, by the fact that it is the only one listed above that takes into account the effect on sorption of impacts of carrier gas molecules, which are many orders of magnitude larger than analyte molecules. In addition, the stage of physisorption necessarily precedes chemisorption. In our case, with the high adjusted coefficient of determination obtained in the work (0.996), there is every reason to assume a linear relationship between these two forms in the studied temperature range and low ozone concentrations. As a result of the selection of coefficients, the best parameter $\alpha = 1$ was determined and a relative increase with temperature t (°C) was predicted for the component μ_{part}, if we take the latter as a unit at 50 °C for each concentration C (ppb). At a given concentration C, the relative sorption gain μ_{part} will be determined by the ratio of the multiplier values $1 + WT\left(1 - \exp\left(-bC\exp\left(\frac{Q}{RT}\right)\right)\right)$ in (1) at a given temperature t and at 50 °C (Figure 2, *b*). It can be seen that, increasing with a value of C, the increase in μ_{part} from 50 to 250 °C reaches 17 % for 250 ppb, which indirectly confirms the assumption of the hydrodynamic regime [5]. (In general, the issue of the effect of adsorption on mobility is relevant in terms of creating low-temperature sensors that operate without heating (Carrier Mobility Dominated Gas Sensor, CDGS [9]).

Also, from the formula obtained by regression (see Figure 2, *a*), it is possible to estimate the elementary adsorption energy $\frac{q}{k_{\text{B}}T} = \frac{0.362\cdot 1000}{T} \Longrightarrow q = 362\,\frac{k_{\text{B}}}{e} \approx 0.031\,\text{eV}$, which corresponds in order of magnitude to the adsorption energy for ozone on methane soot ($0.097 \pm 0.050\,\text{eV}$) [10]).

For the first time, the authors applied the approaches of the method of temperature-controlled desorption (TPD)

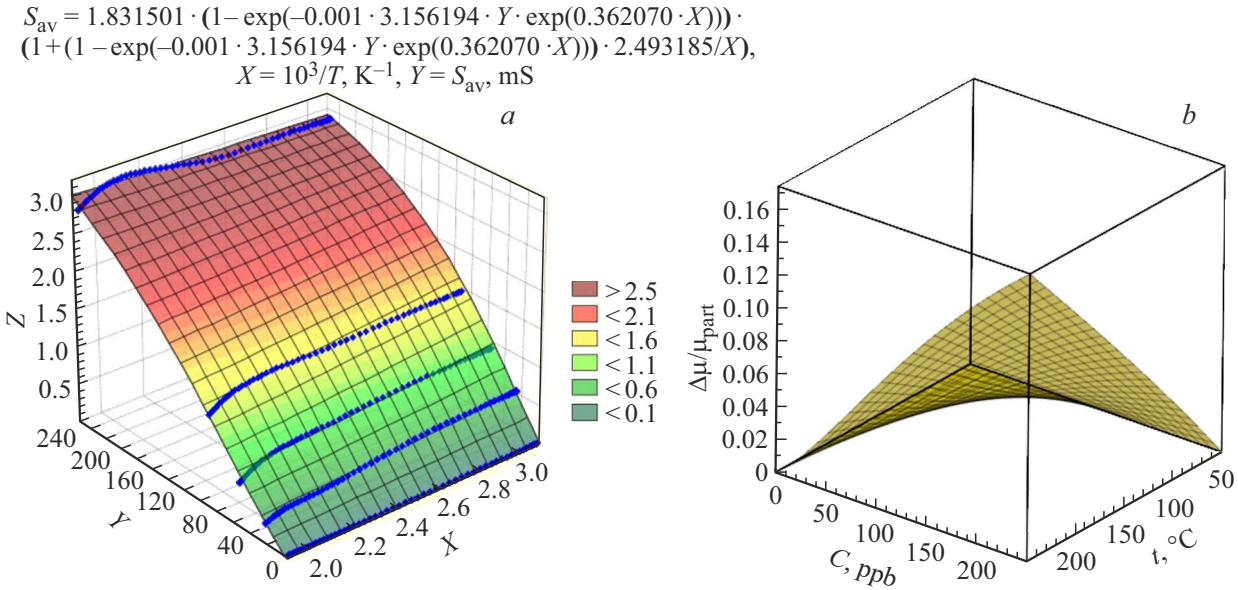

Figure 2. *a* — approximation of $S_{av} = (S_{extr\uparrow} + S_{extr\downarrow})/2$ by the modified Jovanovic formula (1); *b* — forecast according to (1) of relative change of μ_{part} with temperature t (°C) and a concentration C (ppb).

for electrophysical data obtained during the adsorption experiment. In this case, the extracted response S_{extr} played the role of the value of adsorption, and the raw response S played the role of the carrier concentrations.

The basic idea of TPD conductometry is the same as in classical theory: to specify the equation W–P, to determine the desorption mechanism by the degree of the quantities included in its right part, and determine the adsorption according to it. According to the W–P approach, desorption is described by an ordinary differential equation of the 1-st order with respect to time t, rigidly related (usually linearly) with increasing temperature T.

The authors modified the harmonic temperature sweep by linearly relating the inverse Kelvin temperature $1/T$ with time t:

$$\beta_i = \frac{1}{T(t_i, c)} = \frac{1}{T(t_0, c)} - \alpha(t_i - t_0), \quad i = 1, 2, \ldots N. \quad (2)$$

The experiments were carried out with time separation: first in the air flow (reference experiment), then in the air flow with ozone. In the measuring experiment, the samples were kept in an air flow at an initial temperature of 50 °C to an equilibrium resistance value. After that, one of the ozone concentrations was supplied to the measuring cell using the ozone generator GS-024-25 and the electrical conductivity response was recorded for 1000 s. Then the ozone concentration was lowered to zero and at the same time heating was turned on according to the law (2) from 50 to 250 °C with a sweep of 1000 s. There was no ozone in the air flow in the reference experiment. The signal difference $S - S_{air}$ upon heating was taken as the extracted S_{extr} response of TPD (Figure 3, *a*). The graphs show the extracted electrical conductivity responses S_{extr} from $1/T$ of three different PdO films (#7, 8, 5) with TPD according to (2) for 55 ppb O_3 (Figure 3, *a*). The films were produced under comparable process conditions. All films have qualitatively identical responses, which indicates reproducibility of the results.

Next, the response of sample #7 was modeled (StatSoft Statistica 10, adj $- R^2 > 0.9995$) by a quasi-polynomial of 4th order, then numerically differentiated with a lag of 2, giving the derivative $\frac{dS_{extr}}{d\beta}$.

According to the basic idea of the equation in W–N, this derivative is expressed in terms of the values S_{extr} and S in some algebraic way with coefficients depending on the value $\beta = 1/T$. Using nonlinear regression of the dynamic series of the derivative $\left\{\frac{dS_{extr}(\beta_i)}{d\beta}\right\}$ on the series of values $\{S_{extr}(\beta_i)\}$, $\{S(\beta_i)\}$ and $\{\beta_i\}$ at the level of adj $- R^2 > 0.997$ for the studied samples on all concentrations specify an analogue of the W–P differential equation (DE) with the right-hand side, linear in response values:

$$\frac{dS_{extr}}{d\beta} = -\left(A \exp\left(-\left(U - 10^{-3}\frac{h}{\beta^2}\right)\beta\right) S - 10^3 D \exp(-E\beta)\right)(S_{extr} + n). \quad (3)$$

The multiplier $S_{extr} + n$ can be interpreted as the sum of the increase in the concentration of holes in the volume and electrons in the near-surface layer that do not recombine due to the barrier and/or some selection rules [5]. The expressions in the front bracket can be interpreted as the difference in the flow from the volume to the surface (and vice versa depends on the sign of A) of holes and the injection of electrons from the valence band into the near-surface conduction band.

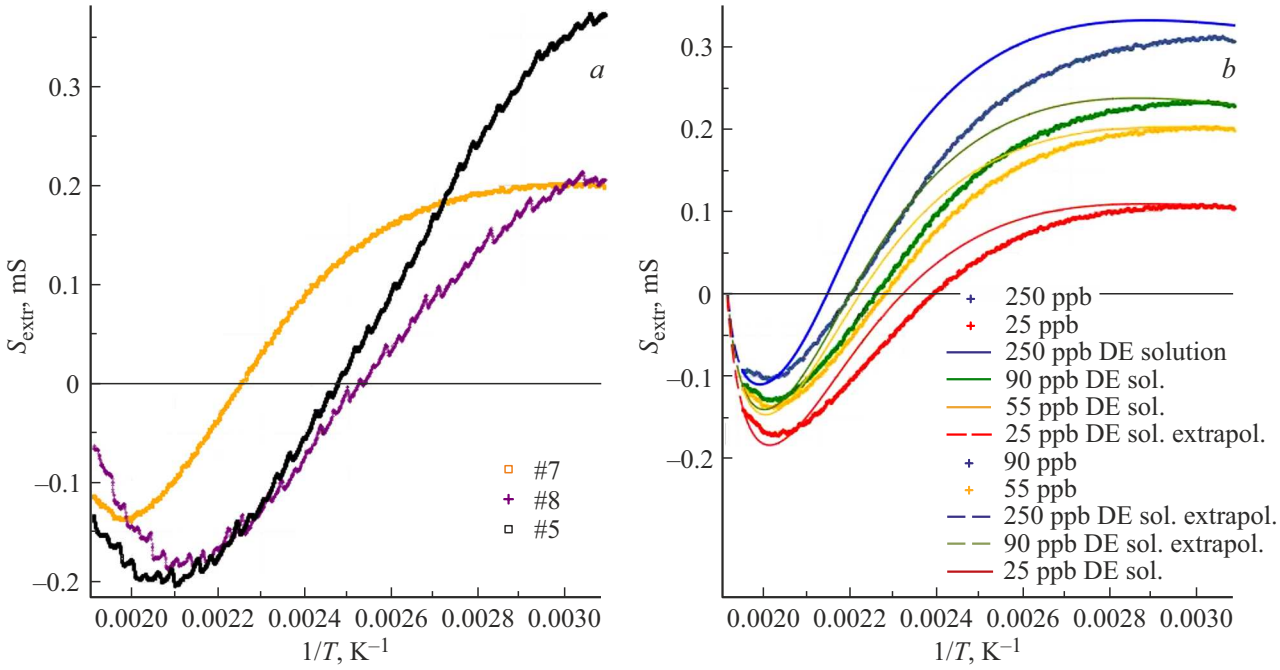

Figure 3. *a* — extracted electrical conductivity responses S_{extr} from $1/T$ of various PdO films (#7, 8, 5) with TPD according to (2) for 55 ppb O_3; *b* — experimental extracted responses at TPD of sample #7 for 4 ozone concentrations, solutions of equation (3) (solid smooth lines) and their extrapolation to zero (dotted line).

Estimates of parameters of DE (3) at different concentrations of O_P3

C, ppb	A	U	h	S_{extr} (50 °C), mS	D	E	n, mSm
0	0	–	–	**0**	0	0	–
25	4.9282	−81	**3.7326**	**0.1040**	**0.1025**	826.4022	**0.6732**
55	6.7105	54.05	**4.063**	**0.1977**	**0.1655**	812.5473	**0.4424**
90	6.094	342.129	**5.645**	**0.2276**	**0.548**	1342.444	**0.373**
250	50.589	1443.188	**6.951**	**0.3057**	**12.864**	2603.045	**0.21**

The linearity of the right-hand side (4) in magnitude S_{extr} may indicate the molecular-ionic form of ozone adsorption or the decomposition of a molecule during adsorption and subsequent desorption due to a triple collision of an ion, a hole, and an O_2 molecule from the gas phase:

$$O_s^- + h_{vol} + O_{2,gas} \rightarrow O_{3,s} \rightarrow O_{3,gas}. \qquad (4)$$

The values of $U - 10^{-3}hT^2$ and E in (3) can be interpreted as additions due to ozone to potential barriers: for holes V_h, decreasing with desorption, and constant 0.23 eV for 250 ppb for electrons V_e. At the same 250 ppb, the value of V_h during desorption drops from 0.06 to a negative value of −0.04 eV, passing through zero in the same place (185 °C), where the line S_{extr} intersects the axis $1/T$ (Figure 3, *b*): $1/T \approx 0.00217\,K^{-1}$.

The specified DE (3) with the substitution of $S = S_{extr} + S_{air}$ for different samples and at different concentrations of O_3 was then checked by numerical integration in Maple 2023 with initial conditions on S_{extr}. The solution of the equation (solid, smooth lines) fit well into the experimental points (Figure 3, *b*). It is also remarkable that their extensions (dotted line) for all concentrations converged on the axis $\beta = 1/T$ at a single point corresponding to $t^{*\circ} = 264\,°C$. Estimates of the parameters of DE (3) at different concentrations O_3 are given in the table.

Of course, there may be doubts about the sign of the values S_{extr} and $\frac{dS_{extr}}{d\beta}$, because the material is of *p*-type, and the analyte is an acceptor. The answer may lie in the fact that the W–P curve is *a priori* nonequilibrium dependence with possible outliers, singularities, etc. for transients. The fact that the extensions of solutions converge at a single point on the axis indicates the expected similarity of the desorption finale for all concentrations of adsorbate.

As for the significantly estimated parameters in (4), those that vary monotonously from C (highlighted in the table) can be used to build a multivariate calibration sensor. It can be seen that these are the parameters h, D, n and the starting value S_{extr} (at 50 °C).

Thus, the chemometric approach provides promising results both in terms of extracting fundamental scientific information and in the purely applied aspect of selective calibration of semiconductor gas sensors.

Funding

The work was partially supported by a grant from the Ministry of Science and Higher Education of the Russian Federation (project No. FZGU-2023-0006).

Conflict of interest

The authors declare that they have no conflict of interest.

References

[1] P. Badica, A. Lorinczi. Coatings, **14**, 1260 (2024). DOI.org/10.3390/coatings14101260
[2] O. García-Serrano, C. López-Rodríguez, J.A. Andraca-Adame, G. Romero-Paredes, R. Pena-Sierra. Mater. Sci. Eng. B, **174**, 273 (2010). DOI: 10.1016/j.mseb.2010.03.064
[3] S.V. Ryabtsev, D.A.A. Gharib, S.Yu. Turishchev, L.A. Obvintseva, A.V. Shaposhnik, E.P. Domashevskaya. FTP, **55** (11), 1034 (2021). (in Russian). DOI: 10.21883/FTP.2021.11.51557.9684
[4] V.V. Chistyakov, S.V. Ryabtsev, A.A.K. Al-Habib, S.M. Solovyov. FTT, **12**, 2107 (2023). (in Russian). DOI: 10.61011/FTT.2023.12.56734.5036k
[5] L. Xu, W. Meng X. Zhang, Xu. Dai, Y. Liu,L. Wang, G. Liu. Phys. Chem. Chem. Phys., **22** (33), 18447 (2020). DOI: 10.1039/d0cp02446e
[6] V.V. Chistyakov, S.A. Kazakov, M.A. Grevtsev, S.M. Solovyov. Pis'ma ZhTF, **6**, 15 (2021). (in Russian). DOI: 10.21883/PJTF.2021.06.50751.18564
[7] J. Estrada-Álvarez, J. Salvador-Sánchez, A. Pérez-Rodríguez, C. Sánchez-Sánchez, V. Clericò, D. Vaquero, K. Watanabe, T. Taniguchi, E. Diez, F. Domínguez-Adame, M. Amado, E. Díaz. Phys. Rev. X, **15**, 011039 (2025). DOI: https://doi.org/10.1103/PhysRevX.15.011039
[8] K.H. Chu, M.A. Hashim, J. Debord, M. Harel, S. Salvestrini, J.-C. Bollinger. Chem. Eng. Sci., **281**, 119127 (2023). DOI.org/10.1016/j.ces.2023.119127
[9] M. Yin, K. Wang, L. Zhang, C. Gao, J. Ren, L. Yu. J. Mater. Chem. C, **11**, 9715 (2023). DOI.org/10.1039/D3TC01551C
[10] V.V. Zelenov, E.V. Aparina. Khim. Fizika, **40** (5), 55 (2021) (in Russian). DOI:10.31857/S0207401X21050149

Translated by A.Akhtyamov